Reports

BioTechniques

An efficient isothermal PCR method for on-site detection of nucleic acid

Shiyin Zhang*[1,2,3], Jin Wang[1,2,3], Zhihao Zhuo[1,2,4], Xiaosong Su[1,2,3], Mengyuan Chen[1,2,3], Wendi Chen[1,2,3], Tingdong Li[1,2,3], Dongxu Zhang[1,2,3], Xiaoping Min[1,2,5], Shengxiang Ge[1,2,3] & Ningshao Xia[1,2,3]

ABSTRACT

Convective PCR (CPCR) is an isothermal nucleic acid amplification technology; however, natural convection exhibits a chaotic and multiplex flow state, resulting in low amplification efficiency and specificity. We placed a polycarbonate strip (p-strip) inside reaction tubes to induce circumfluence by blocking the inner ring that originally allowed fluid to flow at suboptimal temperatures. Moreover, we constructed a dual-temperature instrument to provide appropriate denaturing and annealing zones for CPCR. Tubes containing p-strips exhibited significantly improved efficiency, sensitivity and specificity. For real-time detection, the variation coefficients of three replicates having the same concentrations were less than 2% in more than half of the cases, indicating improved CPCR amplification and potential as a commercial on-site nucleic acid diagnosis tool.

METHOD SUMMARY

Here we propose a new approach that can induce the circumfluence flow according to the setting route by a specially designed tube. There is a polycarbonate strip that served as a flow-barrier hanging in the tube so that the fluid can just pass through the lower or upper zones of the strip. Moreover, the dual-temperature instrument is constructed for providing proper denaturing and annealing zones for CPCR reaction in B-tube.

KEYWORDS

convective PCR • isothermal PCR • molecular diagnostics • point-of-care-test • Rayleigh–Bénard convection

*[1]State Key Laboratory of Molecular Vaccinology & Molecular Diagnostics, Xiamen University, Xiamen, 361102, China; [2]National Institute of Diagnostics & Vaccine Development in Infectious Diseases, Xiamen University, Xiamen, 361102, China; [3]School of Public Health, Xiamen University, Xiamen, 361102, China; [4]School of Life Science, Xiamen University, Xiamen, 361102, China; [5]School of Information Science & Technology, Xiamen University, Xiamen, 361102, China; *Author for correspondence: zhangshiyin@xmu.edu.cn*

BioTechniques 67: 63-69 (August 2019) 10.2144/btn-2018-0190

Nucleic acid detection techniques are important in molecular diagnostics because of their high sensitivity and specificity. However, traditional PCR can only be performed under standardized settings by highly trained staff owing to the complexity of procedures and analysis, long processing time, high energy consumption and bulky and expensive instruments [1]. Microfluidics-based PCR typically forces continuous reagent flow through a meandering path with three different temperature zones. Although this solves the issue of repeated heating and cooling processes, encountered during traditional PCR, the microfluidic chip still requires an extra fluid-driven system and, thus, the bulky instrument problem persists [2]. In the last decades, isothermal amplification techniques, including transcription-mediated amplification, helicase-dependent amplification (HDA), strand displacement amplification, recombinase polymerase amplification, exponential amplification reaction, loop-mediated amplification and nucleic acid sequence-based amplification, have been developed to achieve faster amplification without using complicated thermocyclers [3–8]. However, either a complex primer design or a multiple-enzyme catalytic system limits their widespread use in practical applications [9]. Furthermore, some of these techniques, including HDA, enable amplification at room temperature, which makes their reaction initiation and termination capabilities uncontrollable. This substantially limits their application to nucleic acid quantitative research. Therefore, studies on the efficient performance of controllable amplification, using a simple enzymatic system and portable equipment, have increasingly gained attention in nucleic acid-based diagnostics.

Rayleigh–Bénard PCR (RB-PCR) is a nucleic acid amplification method first proposed by Krishnan *et al.* in 2002 [10]. In this paper, the authors describe a closed reaction chamber consisting of a Plexiglas cylinder with sealed convection cavities sandwiched between a water-cooled top plate and a bottom hot plate at constant temperatures. Using an appropriate chamber diameter/height ratio, the authors established continuous bottom-up temperature gradients via the water-cooled top plate and the bottom hot plate and generated a Rayleigh–Bénard convection flow of the contained liquid. The PCR reagent was sealed in the heated chamber, and the PCR reaction was achieved by repeatedly circulating the PCR reagent through different temperature zones (Figure 1A). As repeated heating and cooling by the thermal cycler is not required, RB-PCR saves time and energy. However, RB-PCR requires a closed chamber, which requires skillful manipulation for certain operations, including loading reagents and sealing both ends without trapping air bubbles. Moreover, contamination is generally unavoidable. To address the drawbacks of RB-PCR, capillary convective PCR (CPCR) was proposed by Chou *et al.* [11]. CPCR uses an open tube instead of the complex chamber module and uses one constant temperature controller for the heat source. For CPCR, the primers are designed based on the principles of a melting temperature (Tm) higher than that at the top of the tube to ensure primer annealing, as well as an amplicon denaturation temperature (Td) lower than that at the bottom of the tube to ensure denaturation. These improvements provide a strong impetus for developing on-site nucleic acid testing methods. ▶

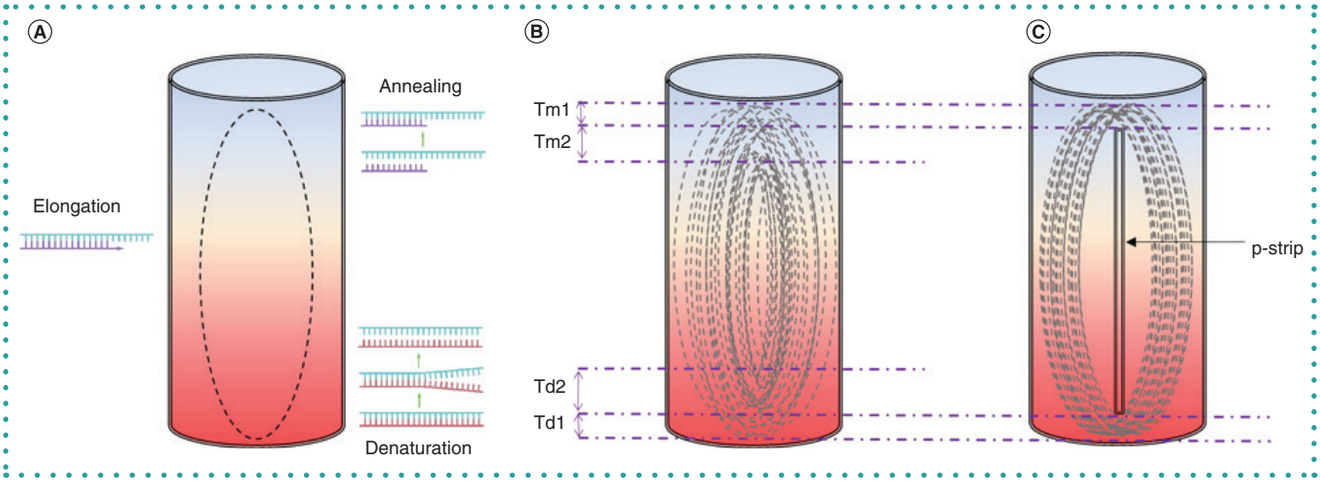

Figure 1. Convective PCR, and flow states of natural or B-tube induced convection. (A) Schematic diagram of convective PCR. When the bottom of a reaction tube is heated, a bottom-up temperature gradient is formed. The reagent at the bottom moves upwards owing to the low density caused by high temperature. Based on the same principle, the reagent at the top moves downward, causing a continuous fluid cycle in the tube. The reagents in the tube circulate spontaneously and undergo the three steps of the PCR cycle as they flow through the corresponding temperature zones. (B) Diagram showing the flow state of natural convection. (C) Diagram showing the flow state in a B-tube.
p-strip: Polycarbonate strip; Td: Denaturation temperature; Tm: Melting temperature.

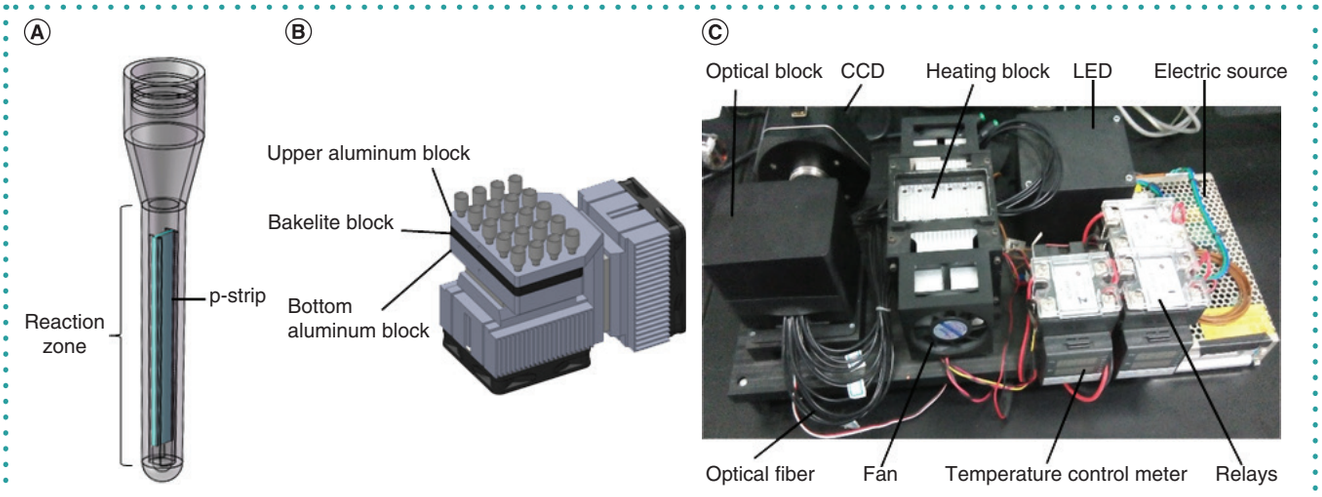

Figure 2. Structure of B-tube and convective PCR instrument. (A) Schematic diagram of the B-tube. The reaction zone of the B-tube is a cylindrical container, and a rectangle p-strip (blue) hangs inside the reaction zone and is fixed by two slots on the inner wall of the tube. (B) Schematic diagram of the dual-temperature instrument for convective PCR (CPCR). The instrument mainly contains two independent heating modules and a bakelite between the two aluminium blocks. (C) Pictures of the real-time fluorescent dual-temperature instrument for CPCR.
CCD: Charge coupled device; p-strip: Polycarbonate strip.

Despite these improvements, no commercial CPCR products have been approved for clinical use over the past 15 years. The major drawback of the method is its low reproducibility, which might be attributed to differing amplification efficiencies among CPCR tubes [12]. Because the largest portion of the CPCR tube was exposed to the surrounding air in early CPCR systems, it was firstly considered that its amplification efficiency could be easily influenced by the environmental temperature. To circumvent this problem, Chang *et al.* developed a device in which aluminum alloy was used as a shield for each tube to baffle the fluctuating surrounding temperature [13]. This significantly reduced the effect of environmental temperature fluctuations and enhanced CPCR reproducibility. In addition, Ahram Biosystems Co., Ltd (Korea) developed a new CPCR module, consisting of three independent heating blocks arranged along the longitudinal axis of the tube, with a gap to avoid heat transfer between the heating blocks [1]. In this instrument, all the PCR reagent-containing zones of the reaction tube were inserted completely into the module, thus reducing the influence of environmental temperature fluctuations. We spent several years on CPCR development for point-of-care use [14–17]. Similar to the instrument developed by Ahram Biosystems, we developed a dual-temperature heating module in our laboratory using bakelite as a thermal insulation layer between the bottom and top heating blocks. This enclosed heating module reduced the

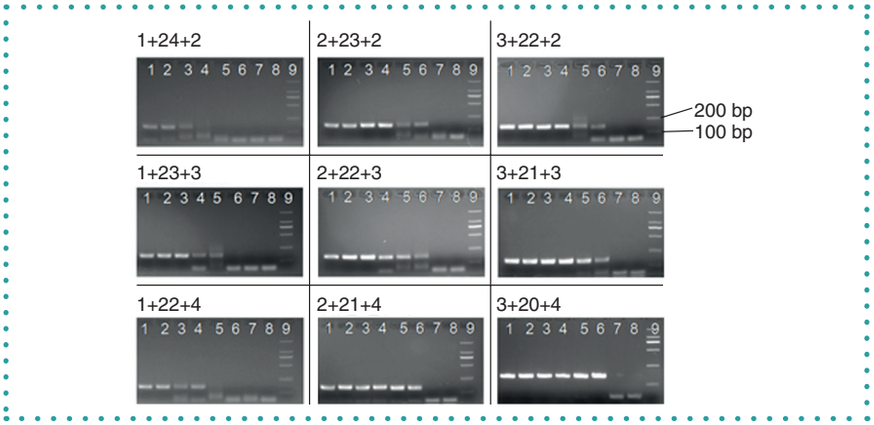

Figure 3. Comparison of nine different polycarbonate strip parameters. As an example, '1+24+2' means the distance between the surface of the reagent and the upper end of the p-strip is 1 mm, the length of the polycarbonate (p)-strip is 24 mm and the distance between the bottom of the B-tube and the lower end of the p-strip is 2 mm. This applies to all parameters. Lanes 1 and 2: 500 copies/test; lanes 3 and 4: 50 copies/test; lanes 5 and 6: 5 copies/test; lanes 7 and 8: negative control; lane 9: DNA marker.

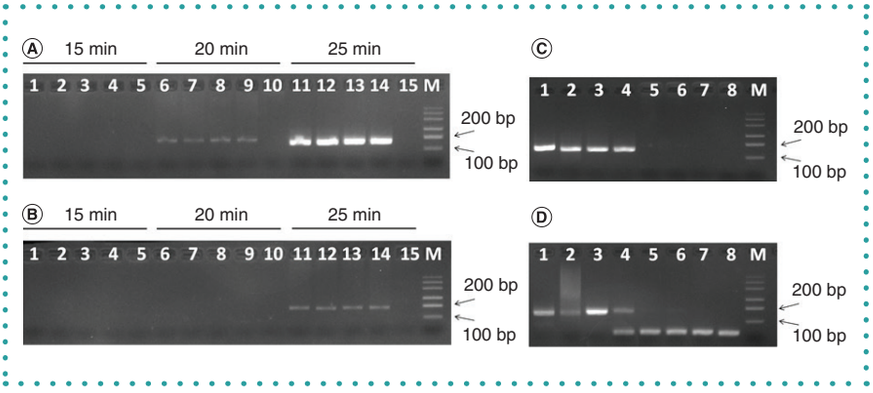

Figure 4. Comparison of amplification efficiency, specificity and reproducibility between B-tube and the tube without a polycarbonate strip. Amplification efficiency of the B-tube (A) and the tube without a polycarbonate (p)-strip (B). Lanes 1–4: positive amplification within 15 min; Lane 5: negative control for 15 min group; Lanes 6–9: positive amplification within 20 min; Lane 10: negative control for 20 min group; Lanes 11–14: positive amplification within 25 min; Lane 15: negative control for 25 min group. Specificity and reproducibility of the B-tube (C) and the tube without a p-strip (D). Lanes 1–4: 5 copies/test; lanes 5–8: negative control; M: DNA marker.

influence of fluctuating environmental temperatures. We then built a portable and miniaturized instrument based on this heating module. The length, width, height and weight of this instrument were 18 cm, 18 cm, 12 cm and 1.5 kg, respectively [18]. However, we still could not achieve a significant improvement in the reproducibility of CPCR amplification.

After that, we noticed that the above improvements focused on providing a relatively stable temperature field from the outside of the reaction tube. However, natural convection showed a chaotic and multiplex flow state inside the reaction tube [11,19], similar to 3D concentric ovals (Figure 1B). As the circulation path influences Td and Tm of each CPCR cycle, the above chaotic and multiplex flow state would have a negative impact on the efficiency, specificity and reproducibility of CPCR. In order to address this drawback in the present study, we initially proposed a new approach that can induce circumfluence according to the route determined by a specially designed tube (B-tube). We placed a polycarbonate strip (p-strip) inside the reaction tubes to induce circumfluence by blocking the inner ring, thus allowing fluid flow through the lower or upper zones of the p-strip (Figure 1C). We used a dual-temperature instrument to provide appropriate denaturing and annealing temperature for the CPCR reaction to occur in the B-tube. We hypothesized that the circumfluence path, along with the specific denaturing and annealing temperature zones, would improve total amplification efficiency and specificity. Thus far, our CPCR system has come very close to satisfying the 'ASSURED' criteria (affordable, sensitive, specific, user-friendly, robust and rapid, equipment-free and deliverable) for the ideal point-of-care testing products proposed by WHO.

MATERIALS & METHODS

Structure of the B-tube

The reaction zone of the B-tube is a cylindrical container with an inside/outside diameter of 2.6 mm/4.0 mm and a length of 27 mm. A rectangle p-strip, 22 mm long, 2.5 mm wide and 0.8 mm thick, hangs inside the reaction zone and is fixed by two slots on the inner wall of the tube (Figure 2A). The volume of the B-tube is 110 μl. After reagent loading, the distance between the surface of the reagent and the upper end of the p-strip is 2 mm, while the distance between the bottom of the B-tube and lower end of the p-strip is 3 mm. The B-tube was produced using a special mould made by Xiamen Voke Mold & Plastic Engineering Co., Ltd (Xiamen, China) according to our design.

Structure of the dual-temperature instrument for CPCR

The dual-temperature instrument has two independent heating modules. Each module uses an aluminium block that tightly surrounds the B-tube to provide suitable Tm and Td from the top (the upper 6 mm in height) and bottom (the lower 8 mm in height) of the B-tube to the reagent. Between the two aluminium blocks, there is a bakelite block, which serves as a shield to isolate the direct heat conduction between the aluminium blocks and is used to reduce the influence of fluctuating environmental temperature to the B-tube (Figure 2B). We measured the temperature inside the tubes using a thermocouple (MS6501, Mastech, China). ▶

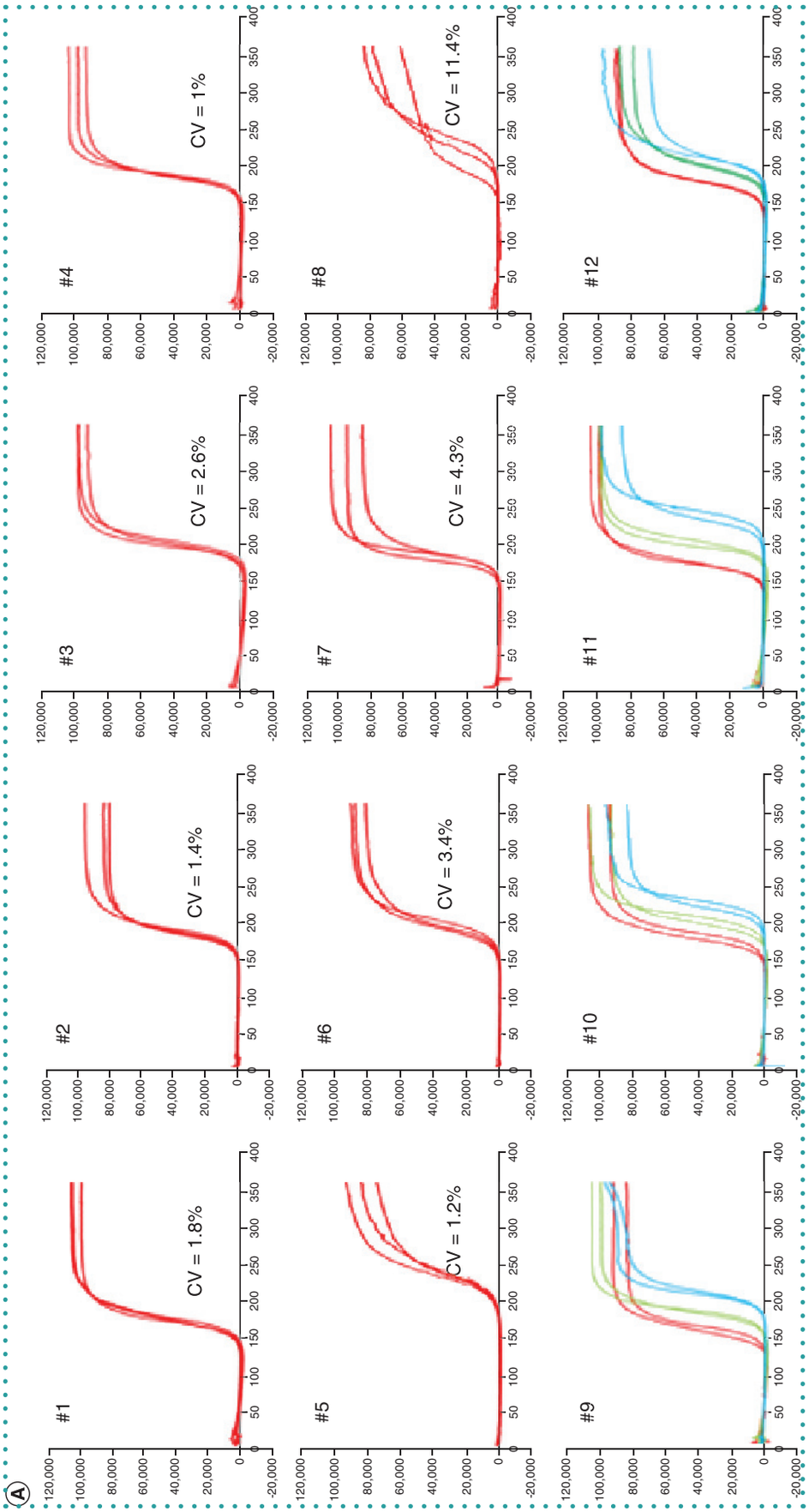

Figure 5. Evaluation of quantitative detection performance of B-tube (also see facing page). (A) Quantitative results of the B-tube. 1–8 show fluorescent curves of eight groups with three replicates of human cytomegalovirus (HCMV) DNA (500 copies/test), 1–7 using B-tubes and 8 using tube without the polycarbonate strip. 9–12 show fluorescence curves of tenfold serially diluted HCMV DNA (500 copies/test [red], 50 copies/test [green] and 5 copies/test [blue]) with two parallel repeats. (B) Fluorescence curves of tenfold serially diluted HCMV DNA (5000 copies/test, 500 copies/test, 50 copies/test and 5 copies/test) amplified using the B-tube. The green dotted lines in (A & B) are the threshold lines with values tenfold that of an SD of 1–100 s. (C) The quantitative correlation between traditional real-time PCR and CPCR with the B-tube.
CPCR: Convective PCR.

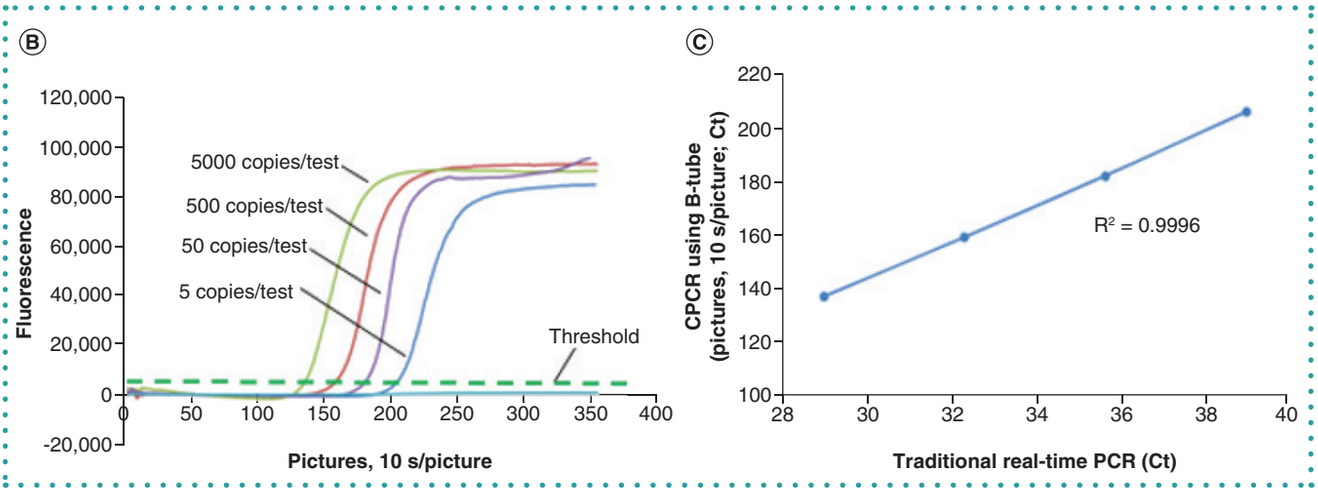

▶ Structure of the real-time fluorescent dual-temperature instrument for CPCR

An optical module was integrated into the above dual-temperature instrument for real-time fluorescence detection. In the module, the excitation light from a LED (XP-E, 450–480 nm, Cree, NC, USA) passed through a filter with 470 nm center wavelength and 30 nm spectral width (Bodian Optical, China) and was then transmitted to the B-tube through an optical fiber (GOFC-S1H-300-P1, Sushi, China). Similarly, the emitted light passed through a filter with 525 nm center wavelength and 20 nm spectral width and was then transmitted to a charge coupled device (CCD; Do3think, China) through an optical fiber (Figure 2C).

Primers & CPCR templates extraction

Primers were designed using Primer3 software (http://www.simgene.com/Primer3). The primers used for human cytomegalovirus (HCMV) were 5′-GTGCGCCTTGACACTGTAC-3′ (forward) and 5′-CGACAAGTACTTTGAGCAGG-3′ (reverse) and for coxsackievirus A16 (CA16) were 5′-CAAGTAYTACCYACRGCTGCCAA-3′ (forward) and 5′-CAACACACAYCTMGTCTCAATGAG-3′ (reverse).

The DNA/RNA extracted from HCMV and CA16 were used as CPCR templates. GenMagSpin Viral DNA/RNA Kit (GenMag, China) was used to purify nucleic acid from the samples according to the manufacturer's instructions. The National Institute of Diagnostics and Vaccine Development in Infectious Diseases conserved the HCMV and CA16 virus strains.

Protocol for CPCR & electrophoresis

The CPCR reaction was performed in the B-tube in a total volume of 110 μl CPCR mixture containing 3.2 mM dNTP (Takara Bio, Japan), 11 μl of 10× Fast Buffer I (Mg^{2+} plus, Takara Bio, Japan), 2 U of SpeedSTAR HS DNA polymerase (Takara Bio, Japan), 1 μl of 10 μM forward primer, 1 μl of 10 μM reverse primer and 20 μl of the nucleic acid template. For amplification from the RNA template (CA16), 0.8 U of AMV Reverse Transcriptase (Promega, USA) was added to the above components. To prevent evaporation, 10 μl of sterile mineral oil (Sigma-Aldrich, MO, USA) was added on top of the reaction mixture. Before amplification, the two heating modules of the dual-temperature instrument were set at 95 and 55°C for accurate Td and Tm, respectively. Next, the B-tube was inserted into the instrument for 30 min for amplification. After amplification, 5 μl of the CPCR product was mixed with 1 μl of 6× loading buffer containing SYBR Green I nucleic acid stain (Invitrogen, USA) and then electrophoresed on a 3.5% agarose (Biowest, Spain) gel in 1× Tris-acetate–EDTA buffer at 180 V for 20 min.

Real-time fluorescence analysis

For real-time fluorescence detection, 5.5 μl of 20× EvaGreen®dye (Biotium, USA) was introduced to the CPCR reaction mixture. The CCD took pictures every 10 s from the beginning of the CPCR reaction. Pictures were imported into the image analysis software developed in the Visual Studio 2013 environment under the Windows system to analyze the sum of the pixel values of each tube. All pixel data were imported into Excel. Because each tube has a different background, the average of the first five data points of each tube was deducted as a background from subsequent data. The processed data were used to generate fluorescence curves using the drawing tool in Excel.

RESULTS & DISCUSSION

Amplification results of B-tubes with different specifications

P-strips with different lengths and positions of tubes were tested. Different parameters, including the distance between the reagent surface and the upper end of the p-strip, as well as the distance between the bottom of the B-tube and the lower end of the p-strip, were tested in cross-combination. In order to obtain appropriate p-strip parameters that could simultaneously exhibit satisfactory sensitivity, specificity and reproducibility, tenfold serially diluted RNA extracted from CA16 (500, 50 and 5 copies/test) were used as RT-PCR templates and ddH_2O was used as a negative control. Results showed that a p-strip length of 20 mm with 3 mm distance to the surface of the reagent and 4 mm distance to the bottom of the B-tube exhibited clear and bright bands even in five copies/test (Figure 3).

Amplification efficiency of the B-tube

The amplification efficiency of the B-tube was tested using three amplification time end points with the same concentrations of HCMV DNA. The time end points were set at 15, 20 and 25 min to determine the amplification speed of the B-tube (Figure 4A) and the control tube without p-strips (Figure ▶

▶ 4B). Amplification bands appeared as early as 20 min in the B-tubes compared to 25 min in the tube without p-strips. At the 25 min end point, B-tube amplification exhibited bright bands; however, tubes without the p-strip only showed weak bands. Comparing the results indicated that the B-tube has better amplification efficiency than the tube without p-strips. As shown in Figure 1B, we assumed that the Td1 region could provide an appropriate denaturation temperature; therefore, the Td2 region, at a higher position than Td1, could not provide the appropriate denaturing conditions. Therefore, in the natural convection state, the double-helix DNA templates that travelled through the Td1 region could be denatured, whereas those that travelled through the Td2 region could not, thus reducing the overall denaturation efficiency. Similarly, for some single-stranded DNA templates and primers that travelled through the Tm2 region with a temperature higher than the annealing temperature, the total annealing efficiency would be low. The designed B-tube could circumvent this problem via the placement of a p-strip inside the tube, which served as a flow barrier and induced circumfluence.

Specificity & reproducibility of the B-tube

The HCMV amplification system was used to evaluate the reproducibility and specificity of the B-tube. Four positive replicates with a low-copy template of five copies/test were amplified using the B-tube and showed bright and homogeneous bands without smears (Figure 4C), while amplification products from tubes without p-strips showed nonhomogeneous bands, as well as smears and primer dimers in two of the replicates (Figure 4D). Similarly, four negative replicates, using the B-tube for amplification, showed a clean background, while tubes without p-strips showed primer dimers. These results demonstrated favorable reproducibility and specificity of the B-tube.

In CPCR, the annealing temperature is usually set lower than the Tm of the corresponding primers to ensure successful annealing between most primers and templates. However, this low-temperature region also provides conditions for nonspecific pairing between primers, between primer and template and with the primer itself, thus producing nonspecific products through elongation. Therefore, CPCR using a tube without a p-strip may show unsatisfactory amplification specificity. In addition, it might cause differences among parallel reaction tubes. For qualitative detection at the end point, the differences reflect different product compositions and composition ratios. Nonspecific CPCR products, such as those described above, would serve as templates in the next amplification round. This would cause an exponential increase in nonspecific amplification products that would, in turn, compete with the correctly amplified template for primers, dNTPs and enzymes. Whether such nonspecific reactions would occur, when they might occur, and the ratio of the occurrence are random and uncontrolled, the earlier the nonspecific amplification occurs, the lower the proportion of correct amplification products in the end point of the reaction.

Quantitative results of the B-tube

First, seven groups of HCMV DNA (500 copies/test) underwent real-time fluorescence quantitative detection using the B-tube for three replicates. Another group using the tube without the p-strip was set as a control. Each group was tested in a different round. Groups tested using the B-tube (Figure 5A, #1–7) showed higher homogeneity than the tube without p-strips (Figure 5A, #8). The coefficients of variation for the seven groups using the B-tube were 1–4.3%, while that of the control was 11.4%.

In order to evaluate the B-tube's quantitative detection potential, four groups of tenfold serially diluted HCMV DNA (500, 50 and 5 copies/test) with two parallel repeats underwent real-time fluorescence quantitative detection. Our findings showed that different templates exhibit regular and distinguishable curves (Figure 5A, #9–12). Next, tenfold serially diluted HCMV DNA (5000, 500, 50 and 5 copies/test) and ddH_2O were tested using the B-tube (Figure 5B) and traditional real-time fluorescence PCR. The quantitative correlation between these two methods was satisfactory for some groups as shown in Figure 5C; however, some groups still showed unsatisfactory quantitative correlation, similar to the above homogeneity tests of #6 and #7.

We noticed that the chaotic and multiplex flow state inside the reaction tube resulted in nonhomogeneous results for qualitative detection. We already know that amplicons in each round act as templates for the next PCR cycle. Therefore, different product compositions caused by insufficient amplification and/or nonspecific amplification during the previous cycle will result in different template numbers for the next cycle of PCR. Therefore, the cycle threshold value would be affected by nonspecific amplification, thus preventing accurate quantification.

In the present study, we found that the CPCR's poor sensitivity, specificity and reproducibility were caused by the chaotic and multiplex flow state associated with natural convection. To address this problem, we designed the B-tube, which has a p-strip hanging in the CPCR reaction area. This little strip organized the fluid state in the reaction tube and guided the reagent to flow through a strictly designed pathway. Although the quantitative performance was not as good as traditional real-time PCR, the efficiency, specificity and reproducibility for qualitative detection of CPCR were significantly improved. In addition, we believe that providing a more regular and uniform fluid state for CPCR is a novel way of determining the rapid fluorescent quantification detection towards commercial use.

FUTURE PERSPECTIVE

Because of the small size and portability of the equipment, as well as its rapid amplification performance and simple operative procedure, CPCR is suitable for use as a point-of-care testing tool. Therefore, we will first establish a cheap and convenient on-site nucleic acid diagnostic platform that combines CPCR with microfluidic nucleic acid extraction. Next, we will engage in providing a more regular and uniform fluid state for CPCR so that it can be used in quantitative detection.

AUTHOR CONTRIBUTIONS

SZ, JW, SG and NX conceived the project; SZ, JW and TL designed the experiment, and wrote the manuscript; SZ, JW, ZZ, XS and MC conducted the behavioural experiment and analyzed the data; WC, DZ and XM designed and fabrication the special equipment.

FINANCIAL & COMPETING INTERESTS DISCLOSURE

This work was supported by the Natural Science Foundation of Fujian Province (grant no. 2017J05136), the National Natural Science Foundation of China (grant no. 8150080605), the National Science and Technology Major Project of China (grant no. 2018ZX10732101–001–002), and the National key research and development program (grant no. 2018YFC1200103). The authors have no other relevant affiliations or financial involvement with any organization or entity with a financial interest in or financial conflict with the subject matter or materials discussed in the manuscript apart from those disclosed.

No writing assistance was utilized in the production of this manuscript.

REFERENCES

1. Zhang S, Xue M, Zhang J *et al.* A one-step dipstick assay for the on-site detection of nucleic acid. *Clin. Biochem.* 46(18), 1852–1856 (2013).
2. Mark D, Haeberle S, Roth G *et al.* Microfluidic lab-on-a-chip platforms: requirements, characteristics and applications. *Chem. Soc. Rev.* 39(3), 1153 (2010).
3. Xu Y, Kim HJ, Kays A *et al.* Simultaneous amplification and screening of whole plasmids using the T7 bacteriophage replisome. *Nucleic Acids Res.* 34(13), e98 (2006).
4. Van Ness J, Van Ness LK, Galas DJ. Isothermal reactions for the amplification of oligonucleotides. *Proc. Natl Acad. Sci. USA* 100(8), 4504–4509 (2003).
5. Ehses S, Ackermann J, Mccaskill JS. Optimization and design of oligonucleotide setup for strand displacement amplification. *J. Biochem. Bioph. Meth.* 63(3), 170–186 (2005).
6. Vincent M, Xu Y, Kong H. Helicase-dependent isothermal DNA amplification. *EMBO Rep.* 5(8), 795–800 (2004).
7. Cook N. The use of NASBA for the detection of microbial pathogens in food and environmental samples. *J. Microbiol. Meth.* 53(2), 165–174 (2003).
8. Piepenburg O, Williams CH, Stemple DL *et al.* DNA detection using recombination proteins. *PLoS Biol.* 4(7), 1115–1121 (2006).
9. Deguo W, Guicheng H, Fugui W *et al.* Drawback of loop-mediated isothermal amplification. *AJFS* 2(7), 83–86 (2008).
10. Krishnan M, Ugaz VM, Burns MA. PCR in a Rayleigh–Bénard convection cell. *Science* 298(5594), 793 (2002).
11. Chou WP, Chen PH, Miao JM *et al.* Rapid DNA amplification in a capillary tube by natural convection with a single isothermal heater. *BioTechniques* 50(1), 52–57 (2011).
12. Almassian DR, Cockrell LM, Nelson WM. Portable nucleic acid thermocyclers. *Chem. Soc Rev.* 42(22), 8769 (2013).
13. Chang HFG, Tsai YL, Tsai CF *et al.* A thermally baffled device for highly stabilized convective PCR. *Biotech. J.* 7(5), 662–666 (2012).
14. Zhang S, Lin Y, Wang J *et al.* A convenient nucleic acid test on the basis of the capillary convective PCR for the on-site detection of enterovirus 71. *J. Mol. Diagn.* 16(4), 452–458 (2014).
15. Qiu X, Ge S, Gao P *et al.* A smartphone-based point-of-care diagnosis of H1N1 with microfluidic convection PCR. *Microsyst. Technol.* 23, 2951–2956 (2016).
16. Qiu X, Zhang S, Mei L *et al.* Characterization and analysis of real-time capillary convective PCR toward commercialization. *Biomicrofluidics* 11(2), 024103 (2017).
17. Krishnan M, Agrawal M, Burns N *et al.* Reactions and fluidics in miniaturized natural convection systems. *Anal. Chem.* 76(21), 6254–65 (2004).
18. Zhuo ZH, Wang J, Chen WD *et al.* A rapid on-site assay for the detection of influenza A by capillary convective PCR. *Mol. Diagn. Ther.* 22(2), 225–234 (2018).
19. Muddu R, Hassan YA, Ugaz VM. Rapid PCR thermocycling using microscale thermal convection. *J. Vis. Exp.* (49), 2366 (2011).